



Size-dependent physicochemical and mechanical interactions in battery paste anodes of Si-microwires revealed by Fast-Fourier-Transform Impedance Spectroscopy



Sandra Hansen ^{a,*}, Enrique Quiroga-González ^b, Jürgen Carstensen ^a, Rainer Adelung ^a, Helmut Föll ^a

^a Institute for Materials Science, Kiel University, 24143 Kiel, Germany

^b Institute of Physics, Benemérita Universidad Autónoma de Puebla (BUAP), 72570 Puebla, Mexico

HIGHLIGHTS

- Mechanical interactions of the silicon inside paste electrodes are crucial.
- Active material loss is accelerated by void formation around silicon.
- Adjustments of binder properties reduce the disassembly of the electrode.
- In-situ, time-resolved impedance spectroscopy monitor physical properties of anode.

ARTICLE INFO

Article history:

Received 15 December 2016

Accepted 5 March 2017

Keywords:

Mechanics

Si microwires

FFT-impedance spectroscopy

Cyclic voltammetry

Charge transfer

ABSTRACT

Perfectly aligned silicon microwire arrays show exceptionally high cycling stability with record setting (high) areal capacities of 4.25 mAh cm^{-2} . Those wires have a special, modified length and thickness in order to perform this good. Geometry and sizes are the most important parameters of an anode to obtain batteries with high cycling stability without irreversible losses. The wires are prepared with a unique etching fabrication method, which allows to fabricate wires of very precise sizes. In order to investigate how good randomly oriented silicon wires perform in contrast to the perfect order of the array, the wires are embedded in a paste. This study reveals the fundamental correlation between geometry, mechanics and charge transfer kinetics of silicon electrodes. Using a suitable RC equivalent circuit allows to evaluate data from cyclic voltammetry and simultaneous FFT-Impedance Spectroscopy (FFT-IS), yielding in time-resolved resistances, time constants, and their direct correlation to the phase transformations. The change of the resistances during lithiation and delithiation correlates to kinetics and charge transfer mechanisms. This study demonstrates how the mechanical and physiochemical interactions at the silicon/paste interface inside the paste electrodes lead to void formation around silicon and with it to material loss and capacity fading.

© 2017 Elsevier B.V. All rights reserved.

1. Introduction

The Commercially available 18650 Li-ion battery cells contain graphite anodes and NCM-spinell cathodes. Those cells have a high cycling stability of over 10,000 cycles but low capacity and therefore are only applicable to low capacity applications. The anode is

based on a rolled-up paste electrode where the graphite material is casted with different ingredients onto a current collector. One of the major problems using graphite anodes next to the low capacity is the exfoliation of the graphite and the ongoing growth of the solid electrolyte interface (SEI). Both properties lead to a significant capacity fading during cycling of the electrode; which makes those batteries not attractive for long-life applications like e-mobility. These problems may be solved by taking micro-structured silicon as an anode material. Compared to graphite electrodes, which have a capacity of only 362 mAhg^{-1} , silicon offers a ten times higher capacity. Micro-structured silicon can withstand high stress caused

* Corresponding author.

E-mail addresses: sn@tf.uni-kiel.de (S. Hansen), equiroga@ieee.org (E. Quiroga-González), jc@tf.uni-kiel.de (J. Carstensen), ra@tf.uni-kiel.de (R. Adelung), hf@tf.uni-kiel.de (H. Föll).

by the volume expansion of Si during lithiation/delithiation without pulverization of the anode [1–3]. While many publications cover silicon thin films or different nano-architectures, this study concentrates on Si microwires as components of a paste electrode.

This is different from previous work where highly ordered Si microwires were arranged in an array anode. Their Cu current collector was deposited in between the wires on one end, guaranteeing a high mechanical stability of the wires and excluding the possible delamination and destruction of the electrode. This kind of Si microwire array ensured a large amount of active material and provided for large cycling stability [4–6] without irreversible losses for over 300 cycles when cycled to 75% (3150 mAhg⁻¹) of their nominal capacity.

Besides the basic type of anode material, the type of electrode i.e. electrode configuration is a crucial parameter when making high performance batteries. Commercially available batteries contain paste electrodes as mentioned above. They are easy to fabricate even on large scale and comparatively cheap. The paste electrode technology is based on a coating or casting process where the slurry (paste of the active electrode material with solvents, conductive additives and binder) is casted homogeneously on a current collector. One major degradation parameter of paste electrodes is the loss of the mechanical or electrical contact between the active material and the copper current collector during volume expansion leading to an increase in the series resistance. The consequence of this is a large capacity fading of those batteries. Another drawback of this type of configuration is their low capacity since the active material is rather diluted. In addition, many degradation factors concerning paste electrodes are not yet fully understood. In order to check for the fundamental physical properties like diffusion and kinetics inside paste electrodes, Si microwire paste electrodes were made by embedding microwires of different sizes into standard pastes. While this compromises the capacity for the reasons mentioned, it allows detailed studies of the process occurring during the (initial) charging and discharging of the battery including the role of the microwire size. From previous studies of these Si microwire arrays, some basic properties about the material are already known and understood allowing easier correlation to mechanisms occurring inside pastes [7,8].

A standard way of analyzing rate-limiting properties inside anodes for Li-ion batteries is Electrochemical Impedance Spectroscopy (EIS). This electro-analytical tool measures the linear response for several frequencies for each frequency individually, thus being time consuming [9–11]. The results are typically displayed in a Nyquist plot but are only useful if only small changes occur during the time of the measurement. EIS is thus quite suitable to analyze open circuit potential or steady state systems but often not fast enough for evaluating dynamic systems like battery anodes.

In-situ Fast-Fourier-Transform Impedance Spectroscopy (FFT-IS) is therefore employed in this study. The linear response for several frequencies is then measured simultaneously and de-convoluted by a FFT. This allows for fast, in-situ impedance analysis [9–11]. Diffusional and ohmic properties of battery electrodes can be identified and studied “in operando”. Fitting the data to suitable RC circuit models produces the time resolution of series and parallel resistances as well as time constants. This kind of representation is new. Several conclusions can be drawn from that time resolution: Every point of the time dependency correlates to a different state of charge or voltage state during the cyclic voltammogram (which is recorded simultaneously). A change in resistance or time constant demonstrate directly changes during lithiation or delithiation. Lithiation and delithiation processes depend directly on the voltages i.e. incorporation voltages [12]. As the voltages are recorded at the same time, the time resolved impedances provide at every

point of the time dependency insights on parameters such as the dependence of diffusion and kinetics on the voltage state and state-of-charge of the battery throughout the measurement.

This study shows the power of the FFT-IS measurement by identifying the most important parameters that influence the battery performance when using Si microwire paste electrodes. It emphasizes that the material parameter of the paste should be considered and discussed in order to avoid unwanted disorientation or destruction of the anode. In addition, it employs different geometries of the microwires since so far it is not known what kind of geometry would be best. The results indicate how diffusion and especially the charge transfer and thus the lithiation and delithiation mechanisms are influenced by the microwire geometry, allowing to identify the “best” size parameters.

2. Experimental

2.1. Etching of Si microwires

In this study, only the essential steps for the fabrication of the microwires are discussed. The details are described in Refs. [8,13,14]. The starting point for the fabrication of Si microwires is a pre-structured Si wafer. Pre-structuring consists of standard lithography as well as dry-chemical etching procedures, which are both not discussed here.

During an anisotropic chemical etching, inverted pyramids are etched into the wafer at the pre-defined points in a periodic array with an exact distance between each other. The pyramids have a sharp tip, needed for the nucleation of the pores then obtained by electrochemical macropore etching [8,15]. Without the structured array of pyramids, a random pore array would result. The electrochemical pore etching is a highly optimized process in terms of electrolyte, passivation and pore structure, and described in detail in Refs. [7,14,16,17]. The pores are anodically etched with a potentiostat by ET&TE GmbH, Kiel. The pores for this study are etched in an electrolyte containing 10 wt % HF, organic solvents and some water. The (somewhat unusual) water in the electrolyte enhances lateral etching and allows producing wider pores. This reduces the etching time of the (time consuming) chemical etching that enlarges the pores until the pore walls meet at the thin parts and microwires are formed. During electrochemical etching the current–time profile must be tailored to the different microwire lengths (= initial pore depths) used in this study. The lengths of the pores vary from 36 μm up to 75 μm. Pore diameters are then enlarged by dissolving the interstices between the pores in a low concentrated KOH etching solution; resulting in a free-standing wire array. Thus, after formation, the wire diameter reduces as a function of time and the over-etching time then must be chosen correctly to obtain the same thickness for each pore lengths. To have the same thickness for the length variation as indicated above the etching time is around 60 min for a thickness of 1.4 μm. Thickness variations of 1.2 μm and 1.8 μm are realized with a process time variation between 30 up to 60 min time.

2.2. Paste electrodes

Si microwires scratched off the Si wafer are mixed with carbon black (CB) and carboxymethyl cellulose (CMC) as binder material. CMC and CB are added to enhance the conductivity of the anode and to hinder a complete disassembly of the anode in a short time. To test the Si microwires without limitations of electronic transport, the weight ratio between the wires and the carbon black is 1:1. In order to avoid the unwanted influence of an additional electrochemically active material like graphite, the used wire paste electrodes contain carbon black. The amount of binder is kept to a

minimum of 10 wt %. This low percentage is sufficient. At higher percentages of CMC, upon volume expansion, the paste delaminates from the current collector leading to complete disassembly. The role of the binder inside the paste is one of the major discussion points of this study, as well as, in the supplementary information [7,18–20]. Fig. 1 shows schematically the paste electrode configuration and an SEM image illustrating how the paste ingredients interact.

Four kinds of paste electrodes were made, differing in the geometry of the Si microwires as follows:

1. Length: 36 μm ; Diameter: 1.4 μm ,
2. Length: 60 μm ; Diameter: 1.2 μm ,
3. Length: 60 μm ; Diameter: 1.8 μm ,
4. Length: 75 μm ; Diameter: 1.4 μm .

Care was taken to keep the mass loading of the wires in the paste constant. This implies, for example, that in pastes with shorter wires, there are more wires. In order to show the influence of a different binder material, the Supplementary Information displays the FFT-IS results of PVDF.

2.3. FFT-IS analysis

Cyclic voltammetry is used to analyze phase transformations in the Si anodes. The voltammograms are recorded within the voltage limits of 1 V and 0.02 V. Unless said otherwise, all the represented data are recorded for five cycles – 1633 min with a sweep rate of 0.1 mV/s. FFT-IS data were recorded simultaneously with the cyclic voltammograms and fitted to an equivalent circuit model. 30 frequencies between 10 Hz and 20 kHz are superimposed and added as a small signal on the dc operation point (dc voltage or current at which the system operates at the particular time of the measurement) [21,22]. The resulting circuit parameters (resistances, capacitances, time constants) are analyzed in real time and can be tentatively attributed to different phenomena inside the battery anode already during the measurements. The equivalent circuit used in this study employs 3 RC circuits (and thus 3 time constants) in series plus a series resistance (see Fig. 3). This model agrees with other works on Si anodes, with the difference that here it is not possible to observe diffusion phenomena (the slowest frequency for the measurement is of 10 Hz, to be able to do it *in operando*). Typical Nyquist plot models are based on two semicircles [23,24] (2

serial RC circuits) considering the SEI formation and the charge transfer kinetics. Gaberscek et al. emphasized in his work the importance of the interfacial contacts. Especially, he demonstrated the direct impedance correlation between the active material and the current collectors at high frequencies [25]. Based on that, this study extends and displays the interfacial effects on silicon microwires. In order to describe all the effects, the mechanics between the active material and the additives are discussed and fitted with an additional semicircle [10,26,27]. The present model describes a series resistance R_s , and three individual parallel resistances R_p and the corresponding capacitances. A standard least square (χ^2 fit) minimization routine is used to fit the impedance data showing a nearly perfect fit of the measured data, i.e. small relative values of χ^2 [28,29].

Fig. 2 shows examples of typical Nyquist plots of the measured data. Those plots are taken at 1 V for every new cycle in order to indicate the changes. Fig. 3 shows the fitting results of the resistances versus time. It indicates how the resistances change in while the cyclic voltage sweeps are performed. The typical Nyquist plots together with an additional inset for better visibility indicate

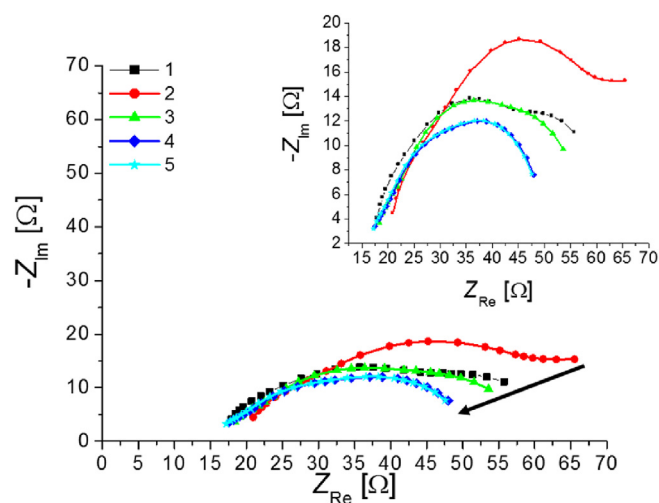


Fig. 2. Example of the change in Nyquist plots obtained from FFT-IS measurements with cycle number. As indicated, the voltammograms are recorded from 1 V to 20 mV and vice versa. The Nyquist plots shown results from every new scan starting at 1 V during the experiments.

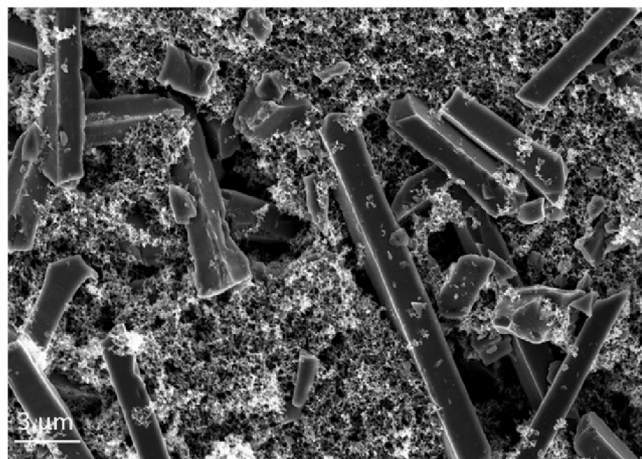
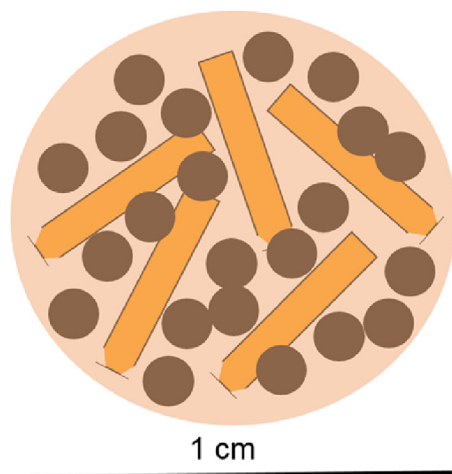


Fig. 1. Structure of Si microwire paste electrode. The SEM image as well as the schematic show how the carbon black covers and embeds the silicon. The binder is not seen but is chemically adsorbed on the silicon.

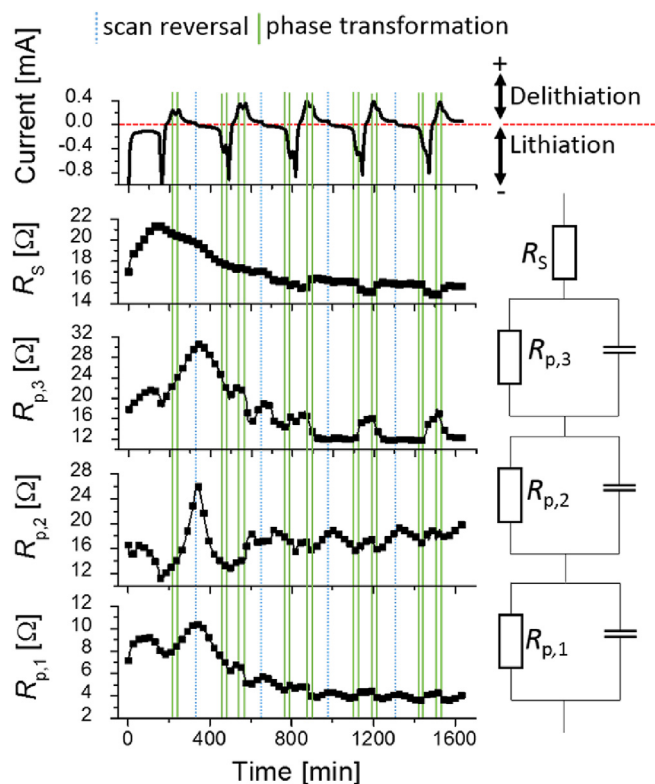


Fig. 3. Example of the resistances in time scale as a result of the FFT impedance spectroscopy during five voltammetry cycles. The recorded current is divided into the delithiation and lithiation currents; showing the partial and full lithiation/delithiation peaks indicated by squares around the phase transformations. On the right side, next to the time dependent behavior of the resistors, the equivalent circuit model is shown. Dashed vertical lines show the scan reversal; whereas solid lines indicate the phase transformations as a guideline for the eyes.

the three semicircles, fitted with the corresponding equivalent circuit. It is clearly seen that the Nyquist plots change their shape with an increasing number of lithiation/delithiation processes. Correspondingly the values of the fitting parameter change, indicating changes of the contribution of the electrochemical processes attributed to the three time constants and resistances. Since the FFT-IS data is recorded every 2 s the changes of all seven fitting parameters is measured almost continuously over time. Thus by comparison e.g. to the time evolution of the characteristic peaks in the voltammogram (indicating physical parameter like phase transformations) the changes in resistances and time constants can be directly related to such physical and chemical effects.

Fig. 2 shows systematic differences in the shape of the curves of the Nyquist plots. These corresponding changes in the Nyquist plots are directly translated into differences in fitting parameters of the corresponding changes during lithiation and delithiation, which are seen in detail in the time-resolved resistances and time constants of **Fig. 3**. The inset shows the re-scaled Nyquist plots for better visibility. With time of cycling, the shape of the Nyquist plots change.

Fig. 3 shows the time dependent dc current of the battery for the first five cycles and the four resistances extracted from the FFT-IS vs. time. A clear time correlation between the resistances and the charge/discharge current is visible. The remaining FFT-IS fitting parameters (capacities, time constants etc.) are not shown here because they would make the graph too busy and most information is extracted from the resistance curves. Sufficient to say that the time data is in agreement with the results extracted from the

resistances.

The series resistance R_s is related to the current collectors and to the counter electrode, which is in a quasi-steady-state by being a semi-infinite Li plate. The resistance is rather small and tends to stabilize to a certain value for lithiation (negative currents) and certain value for delithiation (positive currents) after the first three cycles. After the first three cycles, the SEI stabilizes and the demand of Li from the Li counter electrode also stabilizes, thus its resistance ($R_{p,2}$) tends to stabilize. The origin of the other two resistances, according to previous reports, may be related to the matrix in which the Si wires are immersed and the electrolyte ($R_{p,1}$), and to the charge transfer to the Si wires ($R_{p,3}$) respectively [7,8,30]. The focus here is on the influence of the wire geometry and the order of the wires inside the anode and discusses the mechanical interaction between binder and silicon inside the paste. For the following discussion, the FFT-IS analysis is used as analyzing tool to support that geometry inside anodes matters [12]. Different wire geometries are used (lengths of $l_1 = 36 \mu\text{m}$ to $l_3 = 75 \mu\text{m}$ and thicknesses $th_1 = 1.2 \mu\text{m}$ to $th_3 = 1.8 \mu\text{m}$) allowing to learn more about the reasons for the exceptionally high performance of Si microwires.

3. Results and discussion

The voltammetry results indicate for all the wires a two-step lithiation and delithiation mechanism. The peaks (minima and maxima) represent phase transformations that correlate directly to those Li_xSi_y alloys that correspond to the largest incorporation of Li in Si [6,31].

We have already shown by voltammetric measurements that the length and thickness of the Si microwires influences the battery performance even for nominally identical Si volumes [7].

The phase transformations depend on the length and thickness of the active material, facilitating or hindering the lithiation [12,32,33].

Shorter and thicker unlithiated wires present lower lithiation potentials and smaller operation voltage ranges. For cycling experiments, it is of essential value to know the correct voltage limits, otherwise the battery performance is limited. The perfectly aligned silicon microwire array anodes show exceptionally high cycling performance. They have a different geometry and order, but as well the processes are slightly different compared to a paste electrode with randomly distributed wires. In order to learn more about the wires but also to study paste electrodes, the discussion of the time constants will consider on these topics.

3.1. Parameter dependency on the length of the Si microwires inside paste electrodes

Kinetics involve time constant and the three $\tau = RC$ will be in the focus here. In order to elucidate how the length of the Si wires influences the time constants obtained by FFT-IS, anodes with wires of two substantially different lengths (36 μm and 75 μm ; thickness 1.4 μm) were analyzed.

3.1.1. Interaction between the non-active paste and the silicon microwires as expressed by τ_1 (fastest time constant)

The first and fastest process is correlated to the electrolyte and the interaction between the binder and the active material via the connecting matrix of the paste electrodes. As discussed above, the silicon wires are embedded in a 3D-conducting matrix (carbon black with cellulose) to enhance the conductivity of the active material in the battery. This approach is the standard approach for making paste electrodes. **Fig. 4** shows the time dependent behavior of the first parallel resistance and the correlated time constant for anodes with two different lengths.

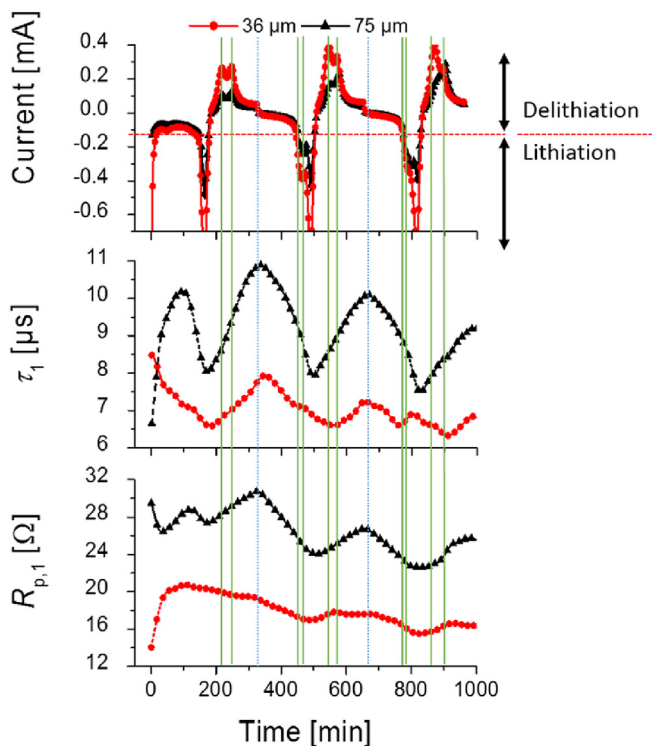


Fig. 4. Comparison of the changes of the parallel resistance $R_{p,1}$ with time for paste electrodes with 1.4 μm thick and 36 and 75 μm long wires. The resistance change upon lithiation/delithiation is mainly due to the contribution of the electrolyte. Dashed vertical lines show the scan reversal; whereas solid lines indicate the occurrence of phase transformations as a guide for the eyes.

The carbon matrix expands or retracts as well during the volume expansion and contraction of the wires due to the lithiation and delithiation processes. The wires shrink faster than the conducting matrix, creating voids around them [34]. From the time constant τ_1 , substantial information could be gained about binder materials and their interaction with silicon, because it is directly related to the conducting matrix. PVDF only forms a thin net of the polymer around silicon and carbon black. CMC, on the other hand, chemically bind on the silicon surface and directly, mechanically interact with silicon. It stabilizes the silicon wires and the matrix, reducing the disassembly of the electrode [18–20,34,35]. The disadvantage of the fine net of the PVDF is that it leaves large areas of active material uncovered and induces reactions between the electrolyte and silicon, like SEI formation or degradation. During volume expansion, the polymer chains of the PVDF expand as well, creating even larger holes between the active materials and reducing the adhesion to the current collector. Cerbelaud et al. simulated the impact of the carboxymethyl groups on the interaction with silicon. Due to direct particle-particle interaction, they propose that the CMC forms “bridges” to silicon [35]. Those bridges are beneficial during volume expansion because they keep in contact with the microwires and retract them. They have the ability to form as many contacts as possible to silicon, covering the wires and leaving only small areas of active material uncovered.

These results show the importance to consider the mechanical interaction at the silicon/paste interface inside paste electrodes. The properties of the binder are important to consider to reduce this unwanted influence.

The good adhesion to the current collector and between the silicon wires and CMC is mirrored by the time dependent behavior of the time constant τ_1 . The bonds of the CMC tend to retract the

wires; reducing the voids. However, voids still exist, giving room for possible reactions of the electrolyte with silicon. On the other hand, because the wires are not electrically connected to the matrix anymore, they lose their contact to the current collector and the resistance increases (see Fig. 3, during the delithiation process – positive currents). Another contribution to this resistance comes from the electrolyte that penetrates the voids of the matrix. The resistance of the carbon alone is rather low. Even when the resistance of the electrolyte is high, the overall resistance is low, since it contains the parallel contributions of carbon and electrolyte. When comparing anodes containing wires with different lengths, it can be seen that the ones with smaller wires present a slightly slower time constant τ_1 . The amount of silicon is the same in both anodes; however, the anode with longer wires has fewer wires in the paste. Therefore, the connectivity with the carbon matrix and with the electrolyte is different in both anodes. The surface per wire is larger in longer wires; this is why the resistance associated to SEI formation is larger in longer wires. Even when there are more wires in the samples with shorter wires, the resistance is not larger; it is even smaller, since there are more resistances in parallel, (the total resistance is smaller than the smallest parallel resistance). As there are fewer wires per cm^2 in the anode with longer wires, there are larger interconnected carbon sections. The conductivity of the carbon matrix/electrolyte mix is higher in this anode, making also its time constant faster. The time constants as well as the resistance contribution show a maximum when the potential scan direction is changed. At that position, the voltage scan changes from delithiation to lithiation. This occurs because the largest void volume is reached when the wires reach the highest level of delithiation (their lowest amount of Li inside). A minimum is obtained at the transitions from lithiation to delithiation.

3.1.2. SEI formation around Si microwires as expressed by τ_2

$R_{p,2}$ is attributed to the formation of the SEI, which forms in the first cycles. It is a passivation layer that is formed on the anode, which hinders the direct contact between the anode and the electrolyte. The SEI of course forms as well on the cathode but the point of interest here is the passivation layer on the anode surface. This leads to a stabilization of the current after the first cycles. This SEI is formed at around 0.7–0.8 V, which is seen by an increase in the current [7]. The electrolyte for the batteries in this study is the standard LP30 (BASF). It contains 11.8 wt % LiPF₆ diluted in ethylene carbonate (EC) and dimethyl carbonate (DMC) [36].

The paste electrodes are made of a carbon matrix partially covering the silicon wires (compare Fig. 1). It is well known that graphite in a battery influences the SEI formation. As a coating i.e. mixed in a paste, the carbon shows a retarding effect on the dissociation of the electrolyte. With its low (electrochemical) reactivity at low potentials, it reduces the formation of fluorine by-products like HF (which might form by reaction of the salt and moisture) [37–39]. The carbon black used in this study has the same effect. The time constant τ_2 , related to the SEI formation, is faster for this paste electrodes than for non-paste electrodes [8].

The resistance $R_{p,2}$ in Fig. 5 shows a clear correlation between the time and the current. The dashed lines emphasize the change in the behavior, which is directly correlated to the change of the current during the potential scan. After reaching a second maximum in the second cycle, the resistance decreases and stabilizes for the rest of the voltammogram. The process of SEI formation produces bigger changes in the resistance in time due to the higher activity in the electrolyte and the reactions at the electrode surface [36,40,41]. After the SEI has been formed, the changes tend to minimize. It is important that $R_{p,2}$ is independent of the phase transformation of the electrodes.

For longer wires, the resistance is higher. This may occur

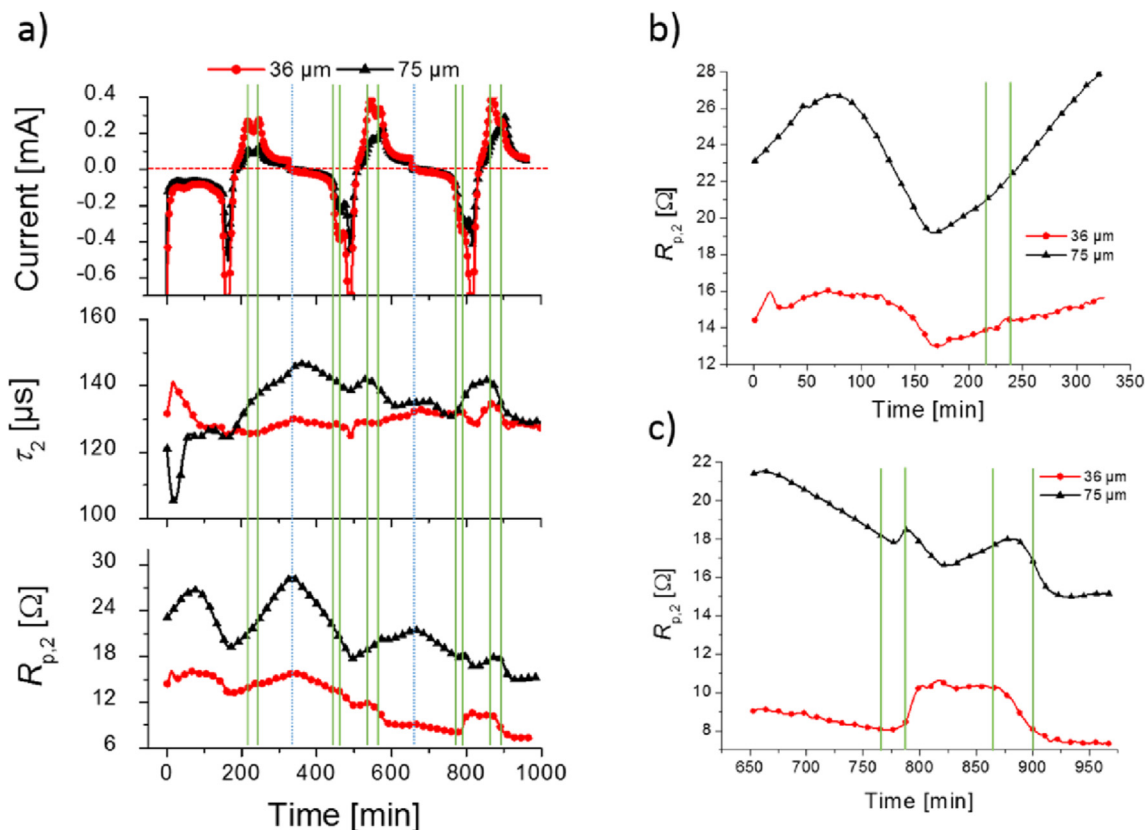


Fig. 5. Comparison of the changes of the parallel resistance $R_{p,2}$ with time for paste electrodes with $1.4 \mu\text{m}$ thick and 36 and $75 \mu\text{m}$ long wires. It shows the contribution of the SEI formation in the resistance change upon lithiation/delithiation. Dashed vertical lines show the scan reversal; whereas solid lines indicate the phase transformations as a guideline for the eyes. a) Total overview of the time dependency. To emphasize the change of the behavior, the first cycle is displayed enlarged in b); the third cycle in c). A second maximum appears with number of cycles because the second phase transformation – the full delithiation – dominates.

because the passivation layer has to be formed over a larger surface area.

With every change of the potential scan (direction) over time, a maximum and minimum develop due to the reaction at the interface with reversal potential. This new reaction leads to a new SEI formation, which leads to an increase in the time constant. Because this reaction has to be performed at longer wires over/across a larger surface area, the time constant and therefore the process is slower. With increasing number of cycles, a second maximum appears (compare Fig. 5c in comparison to the beginning in Fig. 5b) which is more pronounced for longer wires. These could be explained by the enhanced volume expansion and incorporated charges in the silicon wires. This phenomena is indicated in the delithiation peak (partial and fully) where the current increases and the fully delithiation peaks diminishes. The choice of the binder plays an important role. The CMC adsorbs to the wires also over longer distances inside the paste. Upon lithiation, the bonds of the binder elongate leaving room for new SEI formation.

3.1.3. Charge transfer into Si microwires as expressed by τ_3 (slowest time constant)

Fig. 6a shows τ_3 and $R_{p,3}$ over time for five voltammetry cycles. These parameters are related to the kinetics of the slowest process, and can consistently be attributed to the charge transfer into the silicon wires; as it will also be shown below. The time constant τ_3 does not change considerably during the first three cycles in contrast to the corresponding resistance. The following discussion will be centered on the behavior of the resistance $R_{p,3}$. In order to better visualize the change in resistance, the first and fourth cycle

are shown enlarged in Fig. 6b and c. The positions of the current peaks, which are related to phase transformations, are indicated with straight lines in Fig. 6a for an easy correlation.

Comparing the first with the third cycle, a second maximum after the delithiation peaks appears. At a higher percentage of prelithiation (with increasing number of cycles), no new Si–Si bonds have to be broken, the lattice is strained and the incorporation of Li ions becomes easier. More minima and maxima develop near the phase transformations as indicated in the current plot because the second phase transformation is dominating the kinetics (Fig. 6c). During the first cycle (Fig. 6b) where the Li_xSi_y phases start to form (without the formation of lithiation peaks) maxima only appear at the scan reversal. The SEI forms and the Li ions start to incorporate into the silicon anode. The phase transformation i.e. the incorporation of Li into the Si wires is a rather slow process that needs time. In the beginning of the second cycle, these transformations are visible as peaks in the voltammogram. This correlates with the resistance behavior. The resistance increases slightly for short wires, showing a kink at the reversal of the potential scan before it increases further. The increase in resistance is steady without any maxima or minima. SEI formation and the beginning of the alloy formation again dominate the first cycle.

With ongoing lithiation, on the other hand, additional maxima form directly at the peak potentials probably because of a two-step lithiation typical for silicon anodes. Long wires due to their large surface area have more possibilities for the incorporation of charges into the silicon. The (initial) SEI formation is finished and the reversible lithiation and delithiation process occurs. This is also directly indicated in the stable current output. During the third

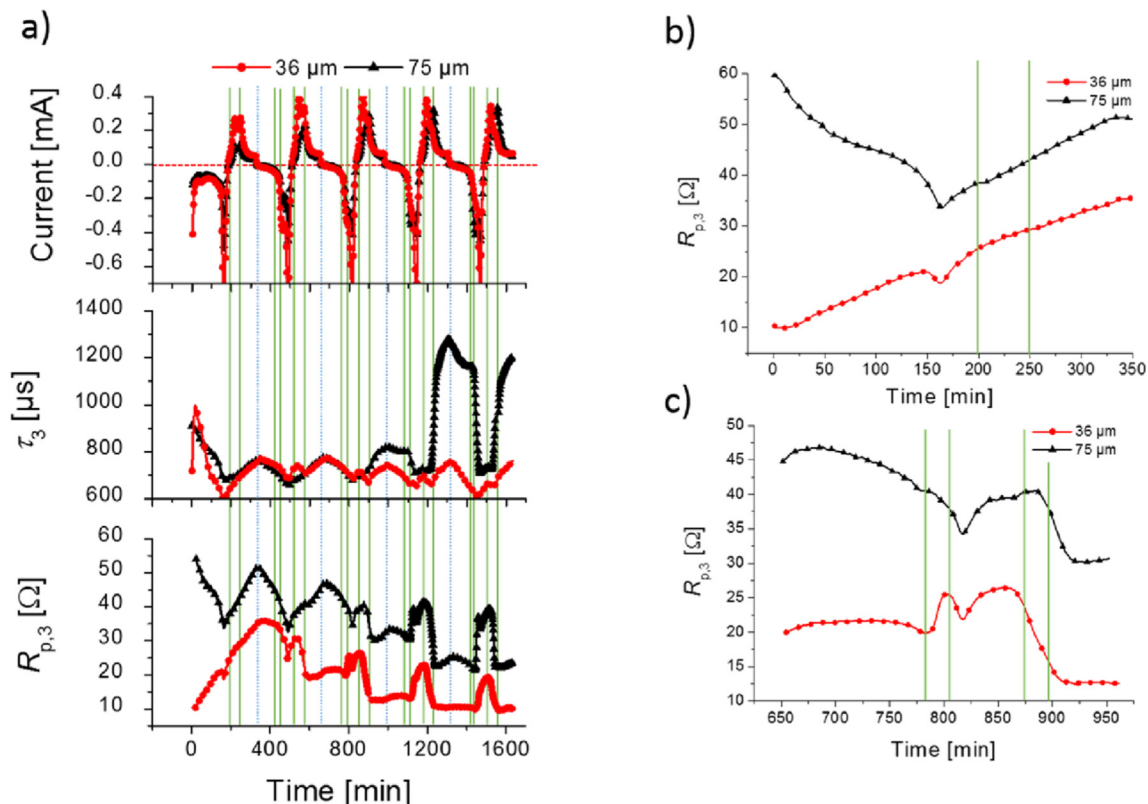


Fig. 6. Comparison of the changes of the parallel resistance $R_{p,3}$ with time for paste electrodes with $1.4 \mu\text{m}$ thick and 36 and $75 \mu\text{m}$ long wires. It shows the influence of the charge-transfer kinetics on the resistance change upon lithiation/delithiation. Dashed vertical lines show the scan reversal; whereas solid lines indicate the phase transformations as a guideline for the eyes. The first and third cycle is displayed as an enlarged inset in b) and c).

cycle (Fig. 6c), a second maximum arises around the second phase transformation. When the ions are incorporated into the anode (with time), the resistance increases every time; not linearly but with every phase transformation. The additional maxima appear exactly due to the enhanced structural changes with time and phase transformation. The phase transformation from crystalline silicon to Li_xSi_y involves the breaking of Si bonds (Fig. 6). In the already lithiated phase, where the delithiation and lithiation process was performed for several cycles, there is a concentration gradient between the Li atoms and the already formed Li_xSi_y phases. This concentration gradient is the driving force for the diffusion across the interface and into the silicon wires. During cycling, the crystal structure of the silicon wires start to change from crystalline to amorphous. In the beginning, only the outer shell of the wires start to amorphize whereas the silicon core stays crystalline. With increasing number of cycles (of pre-lithiation/on-going lithiation), the thickness of the lithiated phase increases changing the crystallinity of the inner core of the wires. After long-term cycling (~ 300 cycles), the wires are completely amorphous. This results in a slower flux and therefore an increase in resistance every time [42–44]. The phases are formed when enough charges at the current potential are incorporated, meaning that the resistance increases steadily before a phase transformation. If the phase transformation occurred, the resistance decreases again to a minimum because no charges are flowing. TXM and TEM measurements (not shown here, since they will be published somewhere else) revealed that the amorphization process highly depends on the C-rate i.e. how fast and under which parameters the wires are lithiated. For slow lithiation processes (for example C/10), the amorphization is very slow in the beginning of the experiment. During the first couple of cycles, only the outer shell (~ 400 nm) of

the wires amorphizes. The inner wire is staying crystalline during these cycles. With ongoing lithiation, tensile stresses attack the SEI layer and the silicon wire leading to delamination of the SEI layer [43].

The direct comparison between both wire lengths shows that the second maximum (with the partial delithiation behavior) forms earlier in shorter wires as in longer wires. As already discussed, more charges could be incorporated in longer wires but it takes longer time to reach phase equilibrium for alloying or Li removal. This is the slowest time constant, since it takes longer to transfer charges between media than to store electronic charge (capacitive effects) or direct electronic conduction.

3.2. Parameter dependency on the thickness of Si microwires in paste electrodes

Additionally to the results discussed above for a wire thickness of $1.4 \mu\text{m}$, the in-situ FFT-IS has been applied to pastes using wires with a thickness of $1.2 \mu\text{m}$ and $1.8 \mu\text{m}$ and a constant length of $60 \mu\text{m}$. When comparing the time constants with the discussion above, it is important to remember that the thickness is different in the wires. Whereas the thickness is kept constant at $1.4 \mu\text{m}$ during the length variation; in the discussion about the thickness variation, only the extrema are discussed.

Fig. 7 shows an overview of the three time constants for the different processes already described in detail above. The time constants differ by three orders of magnitude. The rate limiting process is always the slowest process, which is described by the third process in this study. The slowest process relates to the charge transfer process. Whereas the fastest time constant correlates to the electrolyte flow and the interaction with the matrix. In contrast

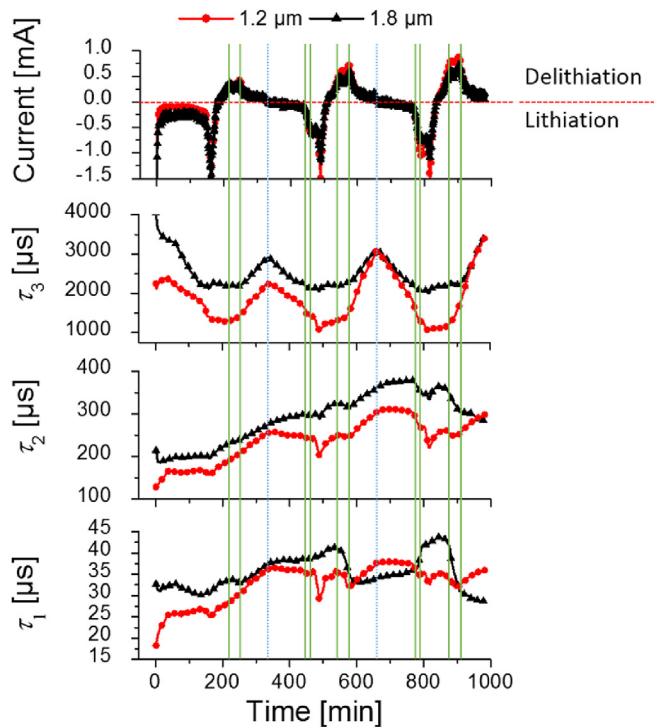


Fig. 7. Comparison of the time constants for paste electrodes with 60 μm long and 1.2 and 1.8 μm thick wires. Dashed vertical lines show the scan reversal; whereas solid lines indicate the phase transformations as a guideline for the eyes.

to the different wire lengths, the first two time constants are slower.

3.3. Interaction between the non-active paste and the silicon microwires as expressed by τ_1 and SEI formation expressed by τ_2

During the phase transformations, Li goes in and out from the anode, causing volume expansions or contractions of the silicon material. As a consequence, the conducting matrix around Si displaces, leaving voids, slowing down the kinetics. This effect is larger in thicker samples. In terms of volume, there are not as many wires in samples prepared with thicker wires as in the ones with thinner wires. This could cause regions in the anode where there are a lot of wires, as well as regions where the carbon black is dominating. Having more voids produces a larger time constant τ_1 . As already discussed in 3.1, τ_1 is attributed to the interaction between the paste and the silicon wires. τ_2 is correlated to the SEI formation. Both processes could be explained together. For different wire thicknesses, the most important characteristic is the increase in the surface area per wire. Due to the larger surface of thicker wires, the SEI has to be formed over a larger surface area producing a larger time constant. In between the phase transformations, the time constants increase for the first as well as for the second processes when the lithiation progresses. The volume expansion is dominant when new ions are incorporated into the wires.

3.3.1. Charge transfer into Si microwires as expressed by τ_3 (slowest time constant)

The rate determining process expressed by τ_3 is discussed in more detail. Fig. 8 shows both the resistance and the time constant of this process, taking always into account the length comparison in Fig. 6.

In the beginning of the measurement, for thickness as well as

length variation, the resistance increases steadily with a maximum when the potential is reversed. During the measurement, when the charge transfer and the formation of the Li_xSi_y alloys stabilizes, maxima and minima in the resistance develop exactly at the time of the phase transformations. With increasing time of the measurement, an additional maximum appears for both thicknesses; but more pronounced for thick wires as shown in the inset of Fig. 8b. These additional maxima form because more charges try to become incorporated into the silicon over time. Due to the increased surface area, more ions could be incorporated into the silicon. When the SEI formation stabilizes, more ions can incorporate and the formation of the Li_xSi_y alloys stabilize. In a previous study [7], the time dependency on the potential was investigated revealing that the incorporation voltages increases with wire thickness. The diffusion of the ions stabilizes after the SEI formation but with increasing number of cycles the internal resistance increases again limiting the diffusional process and increasing the incorporation voltage.

The third time constant shows several maxima and minima, especially at the potential scan reversal but as well around the phase transformations. In general, the process in this comparison is slow. As could be seen in Fig. 8, the thickness is crucial for the time constants (and resistances).

In the length comparison where a medium thickness of 1.4 μm is used, τ_3 increases drastically during the fourth cycle for long wires. Here, in this discussion, a medium length is used and only the thickness is varied and still τ_3 is high. Considering both results, there are co-influences by the thickness and length variation indicating a critical size. Exceeding this critical size, a radial contribution has to be taken into account which influence the process i.e. time constants.

The ions diffuse from every side into the wires, along the side of the wires into the core but also perpendicular to that side. Of course, this happens in every wire configuration. However, very importantly, at this critical size, this process dominates and diffusion only coming perpendicular to the wire i.e. from the middle into wire is present. Still, the core of the wire is not completely lithiated and remains crystalline. When the ions incorporate from the middle and diffuses through the wire, the resistance is smaller because the crystalline core shows enhanced conductivity.

4. Conclusion

Utilizing in-situ FFT-Impedance Spectroscopy it was possible to obtain the time dependent resistances and time constants, which correlate to the diffusional and kinetic changes during lithiation and delithiation processes inside paste electrodes using silicon microwires. Three resistances/time constants could be identified. The fastest process correlates to the electrolyte and the interaction of the silicon during volume expansion. The slowest process in both systems is always the charge transfer kinetics. The formation of the SEI and its role during the interaction in the matrix is also discussed in detail. With this analyzing tool it could be shown that the components in the matrix around the silicon wires like CMC as binder and the conducting agent play an important role in the performance of the battery anode. The function of the binder should not be underestimated.

It is possible to investigate and understand the role of the binder in the interaction with the Si microwires depending on the state of charge of the anode by using time resolving FFT-IS analysis in the fastest time constant. It allows enhancing the understanding of paste electrodes and gives information about the consequences to adapt anode preparation steps.

This study not only reveals the importance of the paste material and its mechanical properties, but also emphasizes the size-dependency of the silicon wires. During long-term cycling

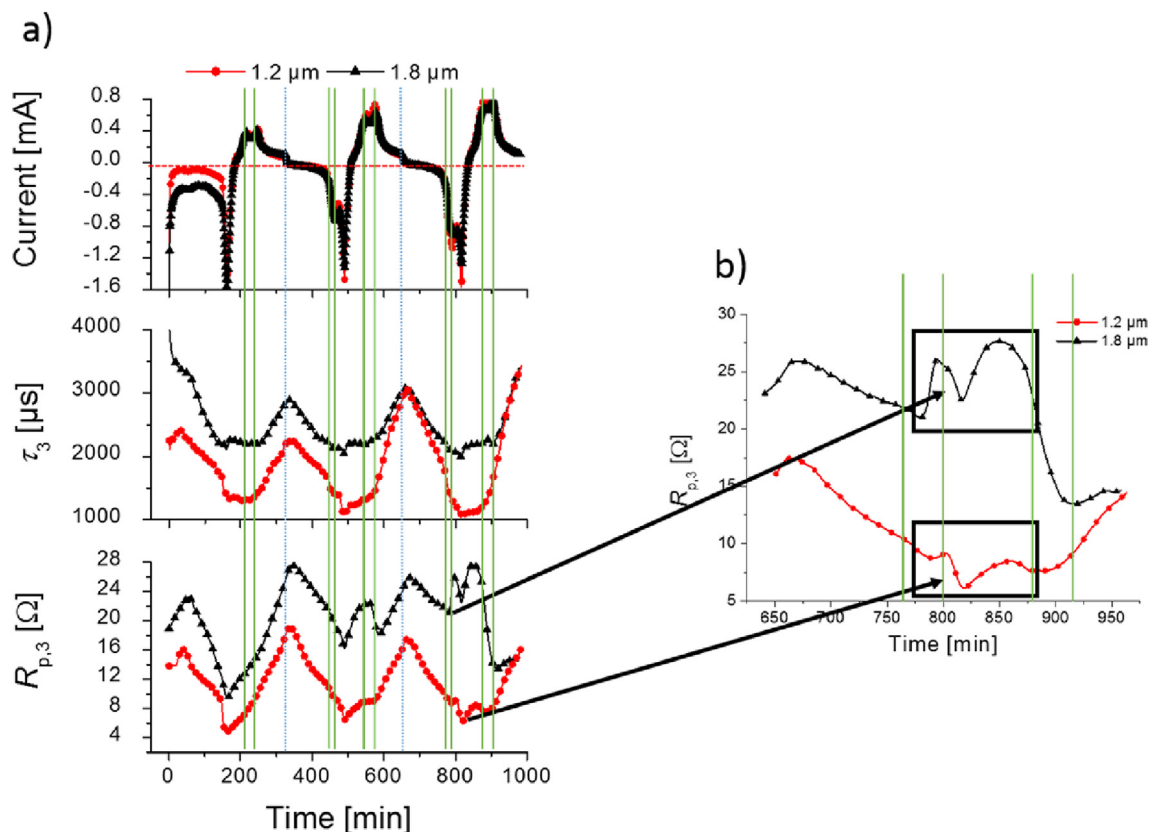


Fig. 8. Comparison the changes of the parallel resistance $R_{p,3}$ with time for paste electrodes with 60 μm long and 1.2 μm and 1.8 μm thick wires. It shows the influence of the charge-transfer kinetics on the resistance change upon lithiation/delithiation. Dashed vertical lines show the scan reversal; whereas solid lines indicate the phase transformations as a guideline for the eye. b) The inset emphasizes the development of a more pronounced second maximum with ongoing lithiation for thick wires.

experiments, the voltage limitation up to which an experiment should be performed is changing according to size. FFT-IS showed what the reason behind that limitation is a difference in the charge-transfer kinetics. A radial contribution has to be taken into account if the Li ions incorporate additionally from the middle of the wire due to the enhanced “absolute” area (like in thick wires for example). As discussed, the outer part starts to amorphize but the inner core stays crystalline. This process is even more dominant in thick wires because here the area of crystalline silicon is larger. With this, more energy has to be provided/overcome to incorporate the ions inside. This additional contribution reduces the time constant. Due to the increased surface area for long wires, the charge transfer has to be along the length of the wire but the connection to the matrix is enhanced because more points are connected. The larger the thickness of the already lithiated phase at the interface, the slower is the flux driven by the concentration gradient of the Li ions. Long wires, on the other hand, profit from their constant thickness. If the interaction and the void formation is less, the charge transfer could be enhanced and stays steadily. If, on the other hand, more voids are formed due to enhanced interaction, larger areas of the active material are exposed to the electrolyte, creating unwanted reactions around the wires. Although short and thin wires have a reduced surface and therefore the amount of charges, which incorporates into the wires is reduced, they may still benefit from their interaction inside the paste.

What is the optimal geometry for silicon anodes? Nobody knows. This study gives first indications of what needs to be considered. It is clear that reducing only one degree of freedom, like the length of a wire, does not result in the best geometry. The thickness, as the second degree of freedom, has to be adjusted too.

Taking this into account, a combination of the best results of this study can be used to find geometries with optimal charge transfer kinetics that are not limited by the surrounding matrix. When deciding for the optimal geometry, it is also important to consider how the processes change with time and state of charge [30]. Here the processes change drastically with the geometry of the wire.

Many factors influencing the battery performance in paste electrodes are not only revealed in this study but quantified to a considerable extent. This allows to understand the various processes influencing electrode performance and to optimize electrodes in a systematic way, taking into account also the role of the electronically “inactive” components of the paste like the binder.

Acknowledgements

This work was supported by the German Research Foundation, who funded this study as part of the project “Elektrochemische und mikrostrukturelle Untersuchung der Prozesse in Anoden für Hochkapazitäts-Lithium-Ionen-Batterien basierend auf Si-Mikrodrahtanordnungen” with grant number FO 258/17-1.

References

- [1] L. Liu, J. Lyu, T. Li, T. Zhao, Well-constructed silicon-based materials as high-performance lithium-ion battery anodes, *Nanoscale* 8 (2016) 701.
- [2] D. Ma, Z. Cao, A. Hu, Si-based anode materials for Li-Ion batteries: a mini review, *Nano Micro Lett.* 6 (2014) 347.
- [3] B. Liang, Y. Liu, Y. Xu, Silicon-based materials as high capacity anodes for next generation lithium ion batteries, *J. Power Sourc.* 267 (2014) 469.
- [4] E. Quiroga-González, J. Carstensen, H. Föll, Optimal conditions for fast charging and long cycling stability of silicon microwire anodes for Lithium ion batteries, and comparison with the performance of other Si anode concepts,

- Energies 6 (2013) 5145.
- [5] L. Mai, X. Tian, X. Xu, L. Chang, L. Xu, Nanowire electrodes for electrochemical energy storage devices, *Chem. Rev.* 114 (2014) 11828.
- [6] C.K. Chan, R. Ruffo, S.S. Hong, R.A. Huggins, Y. Cui, Structural and electrochemical study of the reaction of lithium with silicon nanowires, *J. Power Sources* 189 (2009) 34.
- [7] S. Noehren, E. Quiroga-González, J. Carstensen, H. Föll, Electrochemical fabrication and characterization of silicon microwire anodes for Li ion batteries, *J. Electrochem. Soc.* 163 (2016) A1.
- [8] E. Quiroga-González, J. Carstensen, H. Föll, Structural and electrochemical investigation during the first charging cycles of silicon microwire array anodes for high capacity Lithium ion batteries, *Materials* 6 (2013) 626.
- [9] E. Gileadi, *Physical Electrochemistry - Fundamentals, Techniques and Applications*, Wiley - VCH, Weinheim, 2011.
- [10] E. Radvanyi, K.V. Havenbergh, W. Porcher, S. Jouanneau, J.S. Bridel, S. Put, S. Franger, Study and modeling of the solid electrolyte interphase behavior on nano-silicon anodes by electrochemical impedance spectroscopy, *Electrochim. Acta* 137 (2014) 751.
- [11] R. Ruffo, S.S. Hong, C.K. Chan, R.A. Huggins, Y. Cui, Impedance analysis of silicon nanowire Lithium ion battery anodes, *J. Phys. Chem. C* 113 (2009) 11390.
- [12] S. Hansen, E. Quiroga-González, J. Carstensen, H. Föll, Size-dependent cyclic voltammetry study of silicon microwire anodes for lithium ion batteries, *Electrochim. Acta* 217 (2016) 283.
- [13] E. Quiroga-González, E. Ossei-Wusu, J. Carstensen, H. Föll, How to make optimized arrays of Si nanowires suitable as superior anode for Li-ion batteries, *J. Electrochem. Soc.* 158 (2011) E119.
- [14] E. Quiroga-González, J. Carstensen, C. Glynn, C. O'Dwyer, H. Föll, Pore size modulation in electrochemically etched macroporous p-type silicon monitored by FFT impedance spectroscopy and Raman scattering, *Phys. Chem. Chem. Phys.* 16 (2014) 255.
- [15] V. Lehmann, *Electrochemistry of Silicon*, Wiley-VCH, Weinheim, 2002.
- [16] J. Carstensen, M. Christophersen, G. Hasse, H. Föll, Parameter dependence of pore formation in silicon within a model of local current bursts, *Phys. Status Solidi A* 182 (2000) 63.
- [17] V. Lehmann, S. Rönnebeck, The physics of macropore formation in low doped p-type silicon, *J. Electrochem. Soc.* 146 (1999) 2968.
- [18] A. Magasinski, B. Zdyrko, I. Kovalenko, B. Hertzberg, R. Burtovy, C.F. Huebner, T.F. Fuller, I. Luzinov, G. Yushin, Towards efficient binders for Li-ion batteries Si-based anodes: polyacrylic acid, *ACS Appl. Mater. Interfaces* 2 (2010) 3004.
- [19] B. Lestriez, S. Bahri, I. Sandu, L. Roue, D. Guyomard, On the binding mechanism of CMC in Si negative electrodes for Li-ion batteries, *Electrochem. Commun.* 9 (2007) 2801.
- [20] L. Chen, X. Xie, J. Xie, K. Wang, J. Yang, Binder effect on cycling performance of silicon/carbon composite anodes for lithium ion batteries, *J. Appl. Electrochem.* 36 (2006) 1099.
- [21] J. Carstensen, H. Föll, A. Cojocar, M. Leisner, In-situ FFT impedance spectroscopy in new modes applied to pore growth in semiconductors, *Phys. Status Solidi C* 6 (2009) 1629.
- [22] J. Carstensen, H. Föll, New modes of fast fourier impedance spectroscopy applied to solar materials characterization and semiconductor pore etching, *ECS Trans.* 25 (2009) 11.
- [23] S.S. Zhang, K. Xu, T.R. Jow, Electrochemical impedance study on the low temperature of Li-ion batteries, *Electrochim. Acta* 49 (2004) 1057.
- [24] U. Tocoglu, O. Cevher, T. Cetinkaya, M.O. Guler, H. Akbulut, Cyclic performance study of silicon/carbon nanotube composite anodes using electrochemical impedance spectroscopy, *Acta Phys. Pol. A* 125 (2014) 290.
- [25] M. Gaberscek, J. Moskon, B. Erjavec, R. Dominko, The importance of interphase contacts in Li ion electrodes: the meaning of the high-frequency impedance arc, *Electrochem. Solid State Lett.* 11 (2008) A170.
- [26] J. Guo, A. Sun, X. Chen, C. Wang, A. Manivannan, Cyclability study of silicon-carbon composite anodes for lithium-ion batteries using electrochemical impedance spectroscopy, *Electrochim. Acta* 56 (2011) 3981.
- [27] O.S. Mendoza-Hernandez, H. Ishikawa, Y. Nishikawa, Y. Maruyama, Y. Sone, M. Umeda, State of charge dependency of graphitized-carbon-based reactions in a lithium-ion secondary cell studied by electrochemical impedance spectroscopy, *Electrochim. Acta* 131 (2014) 168.
- [28] B.A. Boukamp, A nonlinear least squares fit procedure for analysis of impedance data of electrochemical systems, *Solid State Ionics* 20 (1986) 31.
- [29] J.P. Meyers, M. Doyle, R.M. Darling, J. Newman, The impedance response of a porous electrode composed of intercalation particles, *J. Electrochem. Soc.* 147 (2000) 2930.
- [30] S. Noehren, E. Quiroga-Gonzalez, J. Carstensen, H. Föll, Dependence of the lithiation/delithiation potentials of silicon microwire anodes on their state of charge and sizes, *ECS Trans.* 64 (2015) 1.
- [31] M.N. Obrovac, L.J. Krause, Reversible cycling of crystalline silicon powder, *J. Electrochem. Soc.* 154 (2007) A103.
- [32] S. Noehren, E. Quiroga-González, J. Carstensen, H. Föll, Fabrication and characterization of silicon microwire anodes by electrochemical etching techniques, *ECS Trans.* 66 (2015) 27.
- [33] R. Chandrasekaran, A. Magasinski, G. Yushin, T.F. Fuller, Analysis of lithium insertion/deinsertion in a silicon electrode particle at room temperature, *J. Electrochem. Soc.* 157 (2010) A1139.
- [34] M.N. Obrovac, V.L. Chevrier, Alloy negative electrodes for Li-Ion batteries, *Chem. Rev.* 114 (2014) 11444.
- [35] M. Cerbelaud, B. Lestriez, D. Guyomard, A. Videcoq, R. Ferrando, Brownian dynamics simulations of colloidal suspensions containing polymers as precursors of composite electrodes for lithium batteries, *Langmuir* 28 (2012) 10713.
- [36] K. Xu, Nonaqueous liquid electrolytes for lithium-based rechargeable batteries, *Chem. Rev.* 104 (2004) 4303.
- [37] L. Fransson, T. Eriksson, K. Edström, T. Gustafsson, J.O. Thomas, Influence of carbon black and binder on Li-ion batteries, *J. Power Source* 101 (2001) 1.
- [38] S. Goriparti, E. Miele, F. DeAngelis, E. DiFabrizio, R.P. Zaccaria, C. Capiglia, Review on recent progress of nanostructured anode materials for Li-ion batteries, *J. Electrochem. Soc.* 257 (2014) 421.
- [39] Y.C. Yen, S.C. Chao, H.C. Wu, N.L. Wu, Study on solid-electrolyte-interphase of Si and C-Coated Si electrodes in lithium cells, *J. Electrochem. Soc.* 156 (2009) A95.
- [40] K.W. Schroder, H. Celio, L.J. Webb, K.J. Stevenson, Examining solid electrolyte interphase formation on crystalline silicon electrodes: influence of electrochemical preparation and ambient exposure conditions, *J. Phys. Chem. C* 116 (2012) 19737.
- [41] J.J. Wu, W.R. Bennett, Fundamental Investigation of Si Anode in Li-ion Cells, NASA Energytech, IEEE, 2012, p. 1.
- [42] M. Pharr, K. Zhao, X. Wang, Z. Suo, J.J. Vlassak, Kinetics of initial lithiation of crystalline silicon electrodes of lithium-ion batteries, *Nano Lett.* 12 (2012) 5039.
- [43] A. Ostadhossein, E.D. Cubuk, G.A. Tritsarlis, E. Kaxiras, S. Zhang, A.C.T. vanDuijn, Stress effects on the initial lithiation of crystalline silicon nanowires: reactive molecular dynamics simulations using ReaxFF, *Phys. Chem. Chem. Phys.* 17 (2015) 3832.
- [44] P. Liu, N. Sridhar, Y.W. Zhang, Lithiated-induced tensile stress and surface cracking in silicon thin film anode for rechargeable lithium battery, *J. Appl. Phys.* 112 (2012) 093507.